AIAA JOURNAL
Vol. 33, No. 8, August 1995

Interlaminar Stresses in General Laminates with Straight Free Edges

Chien-Chang Lin* and Chih-Yu Hsu†
National Chung-Hsing University, Taichung 402, Taiwan, Republic of China
and
Chu-Cheng Ko‡
Aeronautical Research Laboratory, Taichung 407, Taiwan, Republic of China

An efficient analytical method for calculating interlaminar stress distribution near the straight free edges of generally stacked laminates under different types of loading conditions is presented. The variation of stresses for each ply are established according to boundary-layer equilibrium equations. All traction boundary conditions at free edges and traction continuity at ply interfaces are satisfied. Although the emphasis is placed on assessing the behavioral characteristics of interlaminar stresses for unsymmetric laminates, numerical examples for symmetric cases are also presented and compared with available data for demonstrating the efficiency and accuracy of this method. All results show high-stress gradients of interlaminar normal and shear stresses near the free edge.

I. Introduction

IT is well known that stiffness mismatch between adjacent plies of composite laminates causes interlaminar stress concentrations near the traction free edge regions. These stresses will commence delamination damage and may cause the damage to propagate to a substantial region of the laminate resulting in a significant redistribution of stresses and strains.

Numerous investigators[1–9] have used various methods to determine the interlaminar stresses at straight free edge for symmetrically stacked laminates under different types of loading conditions. The first complete three-dimensional analysis of interlaminar stresses in composite laminates was developed by Pipes and Pagano[1] using a finite difference procedure to obtain numerical solutions of the governing elasticity equations. Results were presented for a variety of fiber orientations and stacking sequences. Salamon[2] extended Pipes and Pagano's finite difference techniques for laminates under pure bending. Wang and Crossman[3] proposed a quasi-three-dimensional finite element to obtain the interlaminar stresses in the neighborhood of the free edge. Spilker and Chou[4] studied the same problem using a hybrid-stress finite element model. Chan and Ochoa[5] developed a finite element model for the edge delamination analysis of composite laminates subjected to tension, bending, and torsional loads. Analytical solutions have been obtained by utilizing a variety of techniques including perturbation method,[6] series solution,[7] and Lekhnitskii's complex stress potentials in conjunction with an eigenfunction expansion.[8] In an effort to develop an efficient method to deal with thick laminates, Kassapoglou and Lagace[9] used the force balance method together with the principle of minimum complementary energy to obtain an analytical solution for interlaminar stresses at straight free edges of symmetric laminates.

For most designs of composite laminates, symmetric layup about the midplane are often desirable in order to avoid the coupling effects between bending and extension. However, many practical applications require unsymmetric laminates to specific achieve design requirements. The presence of coupling effects between bending and extension for unsymmetric laminates may substantially change the behavioral characteristics from symmetric cases. Little research effort has been devoted so far in the development of theoretical or numerical models for predicting interlaminar stresses near the straight free edge of unsymmetric laminates. Kassapoglou[10] used the principle of minimum complementary energy in conjunction with calculus of variation to determine interlaminar stresses in general laminates with straight free edges under combined loads. However, no numerical results were given for unsymmetric laminate.

The objective of this investigation is to determine the interlaminar stresses near the traction free edges in generally stacked laminates. The technique developed by Kassapoglou and Lagace[9] for symmetric laminates subjected to uniaxial tension is extended to evaluate the interlaminar stress distribution near the straight free edges of symmetric and unsymmetric laminates under different types of loading conditions. Herein, according to the boundary-layer equilibrium equations, stress variations for each ply are more complex than those assumed by Kassapoglou and Lagace.[9] All of the boundary conditions at free edges as considered in Ref. 9 and traction continuity at the ply interface are satisfied. Numerical results for various unsymmetric laminations are examined to ascertain the influence of bending–extension coupling on interlaminar stress distribution. Good agreement between the present results and available data in the literature for symmetric lamina is also presented.

The analysis presented for determining the interlaminar stress distribution near free edges in generally stacked laminates is simple, and the computational cost is inexpensive. The methodology established should be considered as a very attractive aid in preliminary and detail design phases of composite laminates.

II. Method of Stress Analysis

A generally stacked laminate consisting of N orthotropic plies of equal thickness t subjected to a set of in-plane, bending, and torsional loads in x_1 direction as shown in Fig. 1 is considered. The origin of the local coordinate is located at the center point on the bottom surface of each ply. For the convenience of presentation, a coordinate transformation is introduced as follows:

$$y = b - x_2 \tag{1}$$

The laminate is assumed to be long in the axial x_1 direction. The stress distribution is essentially independent of the x_1 coordinate at a distance sufficiently away from the loading edges. Hence, the equilibrium equations for the kth ply, in the absence of body forces, can be reduced to

$$\begin{aligned} \frac{\partial \sigma_{12}^{(k)}}{\partial y} - \frac{\partial \sigma_{1z}^{(k)}}{\partial z} &= 0 \\ \frac{\partial \sigma_{22}^{(k)}}{\partial y} - \frac{\partial \sigma_{2z}^{(k)}}{\partial z} &= 0 \\ \frac{\partial \sigma_{2z}^{(k)}}{\partial y} - \frac{\partial \sigma_{zz}^{(k)}}{\partial z} &= 0 \end{aligned} \tag{2}$$

Received Sept. 27, 1993; revision received Feb. 28, 1994; accepted for publication Jan. 7, 1995.

*Professor, Institute of Applied Mathematics. Senior Member AIAA.
†Graduate Student, Institute of Applied Mathematics.
‡Associate Scientist, P.O. Box 10008-11.

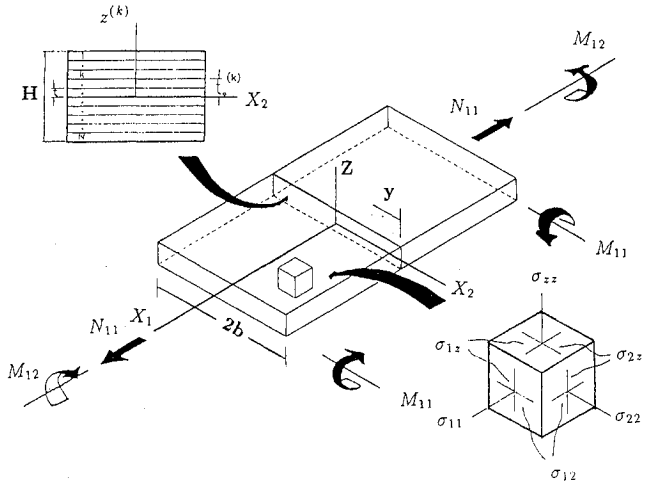

Fig. 1 Laminate geometry and loading conditions.

where $\sigma_{22}^{(k)}$ and $\sigma_{zz}^{(k)}$ are normal stress components and $\sigma_{12}^{(k)}$, $\sigma_{1z}^{(k)}$, and $\sigma_{2z}^{(k)}$ are shear stress components in the kth ply.

A. Stress Functions for Free Edge Region

According to the equilibrium equations (1), stress functions can be developed for a general kth ply by assuming that each stress component, except for $\sigma_{11}^{(k)}$, can be expressed as the product of two independent functions in the following separable form[9]:

$$\sigma_{ij}^{(k)} = f_{ij}^{(k)}(y) g_{ij}^{(k)}(z) \tag{3}$$

Here $f_{ij}^{(k)}(y)$ and $g_{ij}^{(k)}(z)$ are unknown functions to be determined for each ply in the laminate.

Substitution of Eqs. (3) into the equilibrium equations (2) yields the following equations for the unknown functions:

$$\frac{dg_{1z}^{(k)}}{dz} = g_{12}^{(k)} \tag{4a}$$

$$\frac{dg_{2z}^{(k)}}{dz} = g_{22}^{(k)} \tag{4b}$$

$$\frac{dg_{zz}^{(k)}}{dz} = g_{2z}^{(k)} \tag{4c}$$

$$\frac{df_{12}^{(k)}}{dy} = f_{1z}^{(k)} \tag{5a}$$

$$\frac{df_{22}^{(k)}}{dy} = f_{2z}^{(k)} \tag{5b}$$

$$\frac{df_{2z}^{(k)}}{dy} = f_{zz}^{(k)} \tag{5c}$$

The required minimum number of the unknown functions $f_{ij}^{(k)}(y)$ and $g_{ij}^{(k)}(z)$ is four for each ply. The remaining functions can be obtained in terms of the four selected unknown functions by using Eqs. (4a–4c) and (5a–5c) on the condition that boundary conditions and traction continuity at all interfaces are satisfied.

In view of Eqs. (4a–4c), $g_{12}^{(k)}$ and $g_{22}^{(k)}$ are selected as the basic approximate functions in the z direction, the in-plane stress components $g_{12}^{(k)}$ and $g_{22}^{(k)}$ for the free edge region are assumed to vary as linear functions of z,

$$g_{22}^{(k)} = B_2^{(k)} + B_1^{(k)} z \tag{6a}$$

$$g_{12}^{(k)} = B_6^{(k)} + B_5^{(k)} z \tag{6b}$$

Substituting Eqs. (6a) and (6b) into Eqs. (4a–4c), the remaining functions for $g_{ij}^{(k)}(z)$ in the kth ply become

$$g_{2z}^{(k)} = \tfrac{1}{2} B_1^{(k)} z^2 + B_2^{(k)} z + B_3^{(k)} \tag{6c}$$

$$g_{zz}^{(k)} = \tfrac{1}{6} B_1^{(k)} z^3 + \tfrac{1}{2} B_2^{(k)} z^2 + B_3^{(k)} z + B_4^{(k)} \tag{6d}$$

$$g_{1z}^{(k)} = \tfrac{1}{2} B_5^{(k)} z^2 + B_6^{(k)} z + B_7^{(k)} \tag{6e}$$

Similarly, $f_{12}^{(k)}$ and $f_{22}^{(k)}$ are selected as our basic approximate functions of y. Knowing that interlaminar stresses concentrate near the free edge and decay rapidly when moving away from the free edge, $f_{12}^{(k)}$ and $f_{22}^{(k)}$ are assumed to vary as exponential functions of y,

$$f_{22}^{(k)} = A_1^{(k)} e^{-\phi y} + A_2^{(k)} e^{-\phi\lambda y} + A_3^{(k)} \tag{7a}$$

$$f_{12}^{(k)} = A_4^{(k)} e^{-\phi y} + A_5^{(k)} \tag{7b}$$

Substituting Eqs. (7a) and (7b) into Eqs. (5a–5c), the remaining functions for $f_{ij}^{(k)}(y)$ in the kth ply become

$$f_{2z}^{(k)} = -A_1^{(k)} \phi e^{-\phi y} - A_2^{(k)} \phi\lambda e^{-\phi\lambda y} \tag{7c}$$

$$f_{zz}^{(k)} = A_1^{(k)} \phi_1^2 e^{-\phi y} + A_2^{(k)} \phi^2\lambda^2 e^{-\phi\lambda y} \tag{7d}$$

$$f_{1z}^{(k)} = -A_4^{(k)} \phi e^{-\phi y} \tag{7e}$$

The coefficients $A_i^{(k)}$ and $B_i^{(k)}$ given in Eqs. (6a–7e) are to be determined by the associated boundary conditions and interface traction continuities.

B. Boundary and Interface Traction Continuity

The boundary and interface traction continuity conditions of this problem given in Refs. 1 and 9 are as follows.

1) At points away from the free edge region, interlaminar stress components should vanish and stress distribution based on the classical lamination theory should be recovered:

$$\begin{gathered} \lim_{y\to\infty} \left\{\sigma_{1z}^{(k)}, \sigma_{2z}^{(k)}, \sigma_{zz}^{(k)}\right\} = 0 \\ \lim_{y\to\infty} \sigma_{12}^{(k)} = \bar{\sigma}_{12}^{(k)}, \qquad k = 1, 2, \ldots, N \\ \lim_{y\to\infty} \sigma_{22}^{(k)} = \bar{\sigma}_{22}^{(k)} \end{gathered} \tag{8a}$$

here the overbar indicates stresses of classical lamination theory.

2) On the top and bottom surfaces of the laminate:

$$\begin{aligned} \sigma_{1z}^{(1)} = \sigma_{2z}^{(1)} = \sigma_{zz}^{(1)} = 0 \\ \sigma_{1z}^{(N)} = \sigma_{2z}^{(N)} = \sigma_{zz}^{(N)} = 0 \end{aligned} \tag{8b}$$

3) At the interface of two adjacent plies:

$$\begin{gathered} \sigma_{1z}^{(k)} = \sigma_{1z}^{(k+1)} \\ \sigma_{2z}^{(k)} = \sigma_{2z}^{(k+1)}, \qquad k = 1, 2, \ldots, N-1 \\ \sigma_{zz}^{(k)} = \sigma_{zz}^{(k+1)} \end{gathered} \tag{8c}$$

4) At the free edge:

$$\begin{gathered} \sigma_{12}^{(k)} = 0 \\ \sigma_{22}^{(k)} = 0, \qquad k = 1, 2, \ldots, N \\ \sigma_{2z}^{(k)} = 0 \end{gathered} \tag{8d}$$

C. Stress Solutions for Free Edge Region

From classical lamination theory,[11] the midplane extensional strains ϵ_{11}^0, ϵ_{22}^0, and γ_{12}^0 and curvatures κ_{11}, κ_{22}, and κ_{12} for generally stacked laminates can be written in terms of the stress resultants N_{11}, N_{22}, and N_{12} and stress couples M_{11}, M_{22}, and M_{12} as follows:

$$\begin{Bmatrix} \epsilon_{11}^0 \\ \epsilon_{22}^0 \\ \gamma_{12}^0 \\ \kappa_{11} \\ \kappa_{22} \\ \kappa_{12} \end{Bmatrix} = \begin{bmatrix} A_{11} & A_{12} & A_{16} & B_{11} & B_{12} & B_{16} \\ A_{12} & A_{22} & A_{26} & B_{12} & B_{22} & B_{26} \\ A_{16} & A_{26} & A_{66} & B_{16} & B_{26} & B_{66} \\ B_{11} & B_{12} & B_{16} & D_{11} & D_{12} & D_{16} \\ B_{12} & B_{22} & B_{26} & D_{12} & D_{22} & D_{26} \\ B_{16} & B_{26} & B_{66} & D_{16} & D_{26} & D_{66} \end{bmatrix}^{-1} \begin{Bmatrix} N_{11} \\ N_{22} \\ N_{12} \\ M_{11} \\ M_{22} \\ M_{12} \end{Bmatrix} \tag{9}$$

in which A_{ij}, B_{ij}, and D_{ij} are extensional, coupling, and bending stiffnesses, respectively. The presence of B_{ij} implies coupling between extension and bending of a generally stacked laminate.

Using the assumed stress functions given in Eqs. (6) and (7), and the associated boundary conditions given in Eqs. (8a) and (8d), coefficients $A_i^{(k)}$, $B_1^{(k)}$, and $B_5^{(k)}$ can be determined:

$$A_1^{(k)} = -A_2^{(k)}\lambda = -(\lambda/(\lambda-1))A_3^{(k)}$$

$$A_3^{(k)} = \bar{Q}_{12}^{(k)}\left(\epsilon_{11}^0 - t_0^{(k)}\kappa_{11}\right) + \bar{Q}_{22}^{(k)}\left(\epsilon_{22}^0 - t_0^{(k)}\kappa_{22}\right) + \bar{Q}_{26}^{(k)}\left(\gamma_{12}^0 - t_0^{(k)}\kappa_{12}\right)$$

$$A_4^{(k)} = -A_5^{(k)} \tag{10}$$

$$A_5^{(k)} = \bar{Q}_{16}^{(k)}\left(\epsilon_{11}^0 - t_0^{(k)}\kappa_{11}\right) + \bar{Q}_{26}^{(k)}\left(\epsilon_{22}^0 - t_0^{(kd)}\kappa_{22}\right) + \bar{Q}_{66}^{(k)}\left(\gamma_{12}^0 - t_0^{(k)}\kappa_{12}\right)$$

$$B_1^{(k)} = -\left(\bar{Q}_{12}^{(k)}\kappa_{11} + \bar{Q}_{22}^{(k)}\kappa_{22} + \bar{Q}_{26}^{(k)}\kappa_{12}\right)/A_3^{(k)}$$

$$B_5^{(k)} = -\left(\bar{Q}_{16}^{(k)}\kappa_{11} + \bar{Q}_{26}^{(k)}\kappa_{22} + \bar{Q}_{66}^{(k)}\kappa_{12}\right)/A_5^{(k)}$$

here $\bar{Q}_{ij}^{(k)}$ is the ply off-axis stiffness matrix[11] and $t_0^{(k)}$ is the coordinate value from the midplane to the bottom of the kth ply. From the traction continuity conditions at each ply interface given in Eqs. (8c) and traction free conditions at the top and bottom surfaces of the laminate given in Eqs. (8b), the remaining coefficients of $B_i^{(k)}$ can be obtained:

$$B_2^{(k)} = 1$$

$$B_3^{(k)} = \left[\sum_{j=k+1}^{N}\left(\frac{1}{2}B_1^{(j)}t^2 + t\right)A_3^{(j)}\right]\Big/ A_3^{(k)}$$

$$B_4^{(k)} = \left[\sum_{j=k+1}^{N}\left(\frac{1}{6}B_1^{(j)}t^3 + \frac{1}{2}t^2 + B_3^{(j)}t\right)A_3^{(j)}\right]\Big/ A_3^{(k)} \tag{11}$$

$$B_6^{(k)} = 1$$

$$B_7^{(k)} = \left[\sum_{j=k+1}^{N}\left(\frac{1}{2}B_5^{(j)}t^2 + t\right)A_5^{(j)}\right]\Big/ A_5^{(k)}$$

Furthermore, from the interface traction continuity condition, we conclude that ϕ and λ are constants through out the laminate.[9] The final solutions for stresses in the kth ply near the free edge region can be determined as follows:

$$\sigma_{22}^{(k)} = \left(1 + B_1^{(k)}z\right)A_3^{(k)}\left(\frac{1}{\lambda-1}e^{-\phi\lambda y} - \frac{\lambda}{\lambda-1}e^{-\phi y} + 1\right)$$

$$\sigma_{12}^{(k)} = \left(1 + B_5^{(k)}z\right)A_5^{(k)}(1 - e^{-\phi y})$$

$$\sigma_{2z}^{(k)} = \left(\tfrac{1}{2}B_1^{(k)}z^2 + z + B_3^{(k)}\right)A_3^{(k)}\phi\lambda/(\lambda-1)(e^{-\phi y} - e^{-\phi\lambda y})$$

$$\sigma_{1z}^{(k)} = \left(\tfrac{1}{2}B_5^{(k)}z^2 + z + B_7^{(k)}\right)A_4^{(k)}\phi e^{-\phi y}$$

$$\sigma_{zz}^{(k)} = \left(\tfrac{1}{6}B_1^{(k)}z^3 + \tfrac{1}{2}z^2 + B_3^{(k)}z + B_4^{(k)}\right) \times A_3^{(k)}\frac{\phi^2\lambda}{\lambda-1}(\lambda e^{-\phi\lambda y} - e^{-\phi y}) \tag{12}$$

$$\sigma_{11}^{(k)} = \left(\bar{S}_{11}^{(k)}\bar{\sigma}_{11}^{(k)} + \bar{S}_{12}^{(k)}\bar{\sigma}_{22}^{(k)} + \bar{S}_{16}^{(k)}\bar{\sigma}_{12}^{(k)} - \bar{S}_{12}^{(k)}\sigma_{22}^{(k)} - \bar{S}_{13}^{(k)}\sigma_{zz}^{(k)} - \bar{S}_{16}^{(k)}\sigma_{12}^{(k)}\right)\Big/\bar{S}_{11}^{(k)}$$

here $\bar{S}_{ij}^{(k)}$ are anisotropic compliances for the kth ply. It should be noted that the stress component $\sigma_{11}^{(k)}$, which was dropped in equilibrium equations (2), is obtained by using the strain-displacement and strain-stress relationships.[9]

D. Complementary Energy Minimization

It is evident that the problem has been reduced to solve for the unknown parameters ϕ and λ. They are determined through complementary energy minimization. The total complementary energy Π_c in the laminate is

$$\Pi_c = \sum_{k=1}^{N}\Pi_c^{(k)}$$

$$= \sum_{k=1}^{N}\frac{1}{2}\iiint_{V^{(k)}}\sigma^T\bar{S}^{(k)}\sigma\,dV - \iint_{A_u}\boldsymbol{T}^T\bar{\boldsymbol{u}}\,dA \tag{13}$$

here σ is the stress vector, $\bar{S}^{(k)}$ is the kth ply anisotropic compliance matrix, $V^{(k)}$ is the volume of the kth ply, A_u is the area where displacements $\bar{\boldsymbol{u}}$ are prescribed, and $\boldsymbol{T}$ is the surface traction over A_u.

Substituting the stress expressions (12) into Eq. (13) and then taking partial derivatives with respect to ϕ and λ, we obtain the following nonlinear simultaneous algebraic equations:

$$\frac{\partial\Pi_c}{\partial\lambda} = \lambda^4\phi^4 f_2 + 2\lambda^3\phi^4 f_2 + \lambda^2\left\{2(2f_6 + f_9 + f_1) + \phi^2(2f_{11} + f_3 - 2f_{10} - 2f_8)\right\} + \lambda(8f_6 + 8f_9 + 6f_1) + 4f_6 + 4f_9 + 3f_1 = 0 \tag{14}$$

$$\frac{\partial\Pi_c}{\partial\phi} = 3\phi^4\lambda^3 f_2 + \phi^2\left\{\lambda^2(f_4 + 2f_{11} + f_3 - 2f_{10} - 2f_8) + \lambda f_4\right\} + \lambda^2\{f_5 + 6f_9 + 3f_1 + 4(f_7 + f_6)\} + \lambda\{f_5 + 8f_9 + 5f_1 + 4(f_7 + 2f_6)\} + 4f_9 + 3f_1 + 4f_6 = 0 \tag{15}$$

The expressions for f_i are given in the Appendix. The Newton–Raphson iterative method is used to solve Eqs. (14) and (15). There are 16 pairs of ϕ and λ in Eqs. (14) and (15). However, only one pair that has positive real value is needed in minimizing the complementary energy. A detailed iterative algorithm for solving ϕ and λ given in Ref. 9 is followed in the present analysis.

III. Numerical Results and Discussions

To check the accuracy and efficiency of the present method, numerical results are compared to data available in the literature. Material properties with respect to principal material axes of each ply for the high-modulus graphite/epoxy given in Refs. 1, 3, and 5 are used. They are $E_{11} = 20.0$ Msi, $E_{22} = E_{33} = 2.1$ Msi, $G_{12} = G_{13} = G_{23} = 0.85$ Msi, $\nu_{12} = \nu_{13} = \nu_{23} = 0.21$, and $t = 0.005$ in. For the purpose of assessing the accuracy of this method, laminates with $(0/90)s$, $(45/-45)s$, and $(0_2/\theta_2)s$ under a uniform axial strain $\epsilon_{11} = 10^{-6}$ and a prescribed curvature $k_{11} = 0.1$, respectively, are

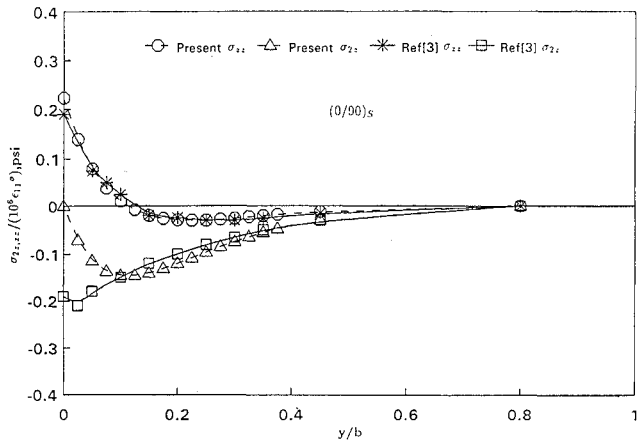

Fig. 2 Interlaminar stresses σ_{2z} and σ_{zz} distribution along the 0/90 interface of a (0/90)s laminate under tension.

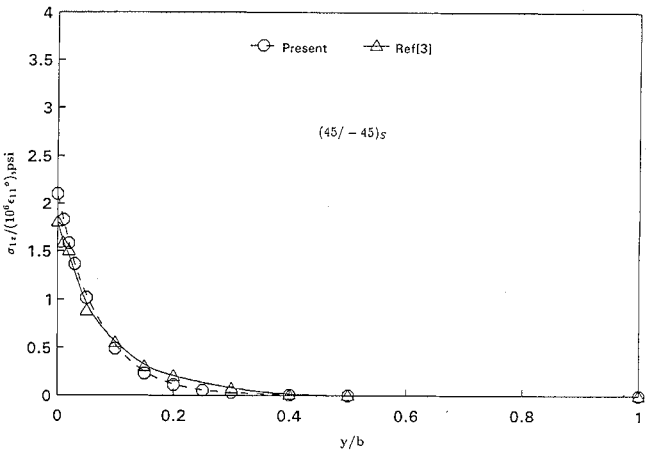

Fig. 3 Interlaminar stresses σ_{1z} distribution along the 45/−45 interface of a (45/−45)s laminate under tension.

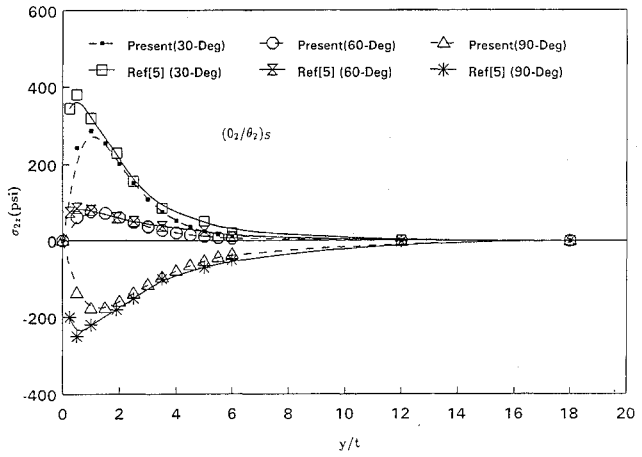

Fig. 4 Interlaminar shear stress σ_{2z} distribution along the upper 0/θ interface of $(0_2/\theta_2)s$ laminates under bending.

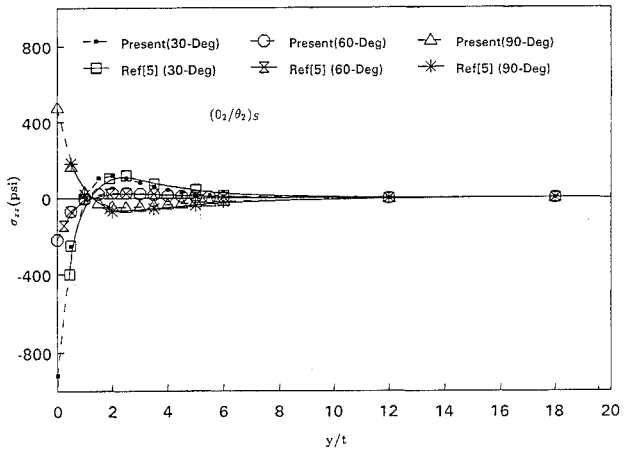

Fig. 5 Interlaminar normal stress σ_{zz} distribution along the upper 0/θ interface of $(0_2/\theta_2)s$ laminates under bending.

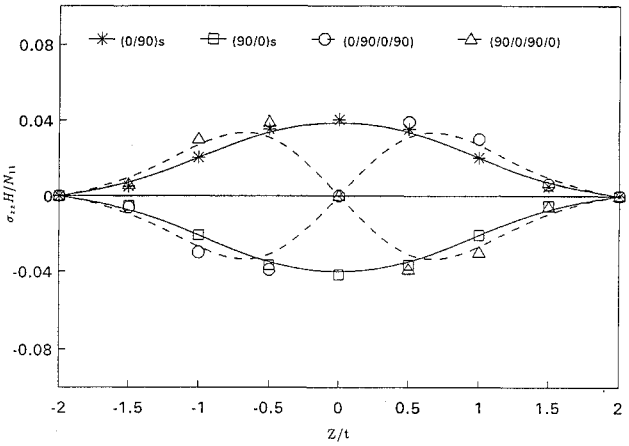

Fig. 6 Through-the-thickness distribution of interlaminar normal stress σ_{zz} at free edge.

considered. Results from the present method for the distributions of interlaminar stress σ_{zz}, σ_{2z}, and σ_{1z} across the width at interfaces between 0 and 90 deg, and +45-deg and −45-deg plies for the top two plies of the laminate are compared with those by Wang and Crossman[3] as shown in Figs. 2 and 3. Aside from σ_{2z}, for which the boundary condition on σ_{2z} at the free edge location are different between the analysis in Ref. 3 and that considered in the present analysis, present results agree well with those given in Ref. 3. The interlaminar normal stress σ_{zz} and shear stress σ_{1z} all exhibit high-stress gradients near the free edge indicating that these stresses have the tendency of being singular at the free edge location. Figures 4 and 5 show good agreement of the present results with those of Chan and Ochoa[5] on interlaminar shear stress σ_{2z} and normal stress σ_{zz} at the interface between 0 and θ deg of the top two plies of $(0_2/\theta)_S$ laminates with the angle θ varying at every 30-deg interval. Again, results of σ_{zz} exhibit a high-stress gradient near the free edge along the interface indicating that the stress σ_{zz} has the tendency of being singular at the free edge location.

To investigate the effect of stacking sequence on the interlaminar normal stress at the free edge due to uniaxial tension, several laminates synthesized by the ply groups of (0/90) were analyzed. The laminates considered were (0/90)s, (90/0)s, (0/90/0/90), and (90/0/90/0). Figure 6 displays the distribution of interlaminar normal stress σ_{zz} through the thickness of the laminate at the free edge location. It is seen that σ_{zz} in these laminates reach their peak values at different interfaces. The contrast of the shape of the curves for these laminates is also remarkable. For (0/90)s and (90/0)s laminates, the variation of σ_{zz} is symmetric about the midplane of the laminates. However, the variation for (0/90/0/90) and (90/0/90/0) laminates are antisymmetric. This reveals that these four laminates exhibit fundamentally different behavior.

The case of antisymmetric angle ply laminates ($\theta/-\theta/\theta/-\theta$) subjected to uniaxial tension is analyzed. The effect of laminate angle θ on the free edge interlaminar stress is assessed by comparing the variation of interlaminar stresses σ_{1z} and σ_{zz} at the free edge location. As shown in Fig. 7, both interlaminar stresses σ_{1z} and σ_{zz} reach their maximum values at the midplane of the (40/−40/40/−40) laminate.

Finally, the effect of laminate thickness on the free edge stresses was investigated by analyzing the ($\theta/90_n/90_n/0$) laminates subjected to uniaxial tension. In Figs. 8 and 9, the distribution of interlaminar shear stress σ_{1z} at the interface between θ-deg and 90-deg plies and the normal stress σ_{zz} at the midplane of the laminates are presented as a function of laminate angle θ varying at every 10-deg

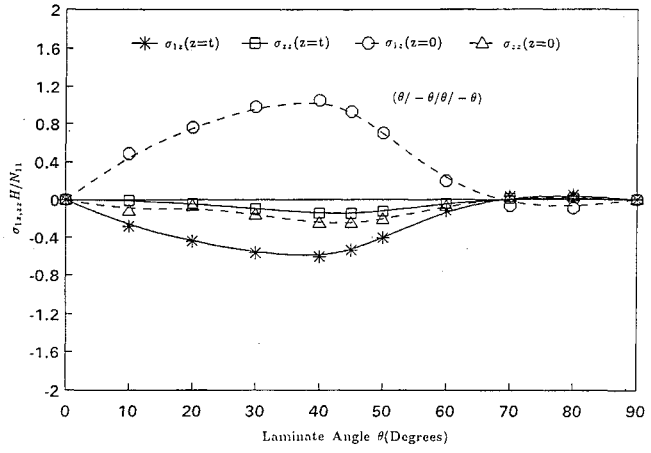

Fig. 7 Interlaminar stresses σ_{1z} and σ_{zz} distribution of antisymmetric $(\theta/-\theta/\theta/-\theta)$ laminates under tension.

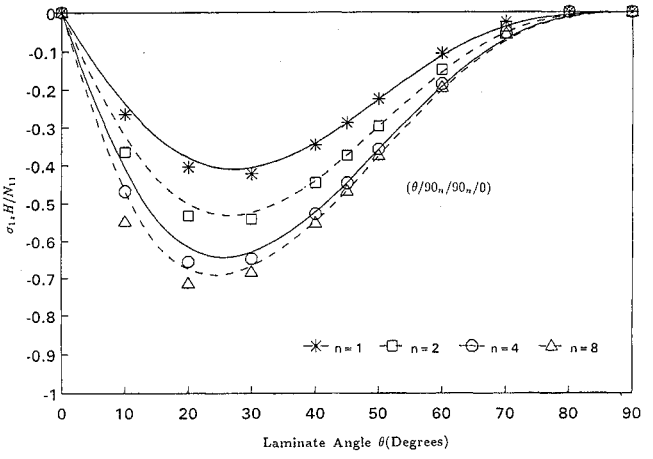

Fig. 8 Interlaminar shear stress σ_{1z} distribution along the upper $\theta/90$ interface of $(\theta/90_n/90_n/0)$ laminates under tension.

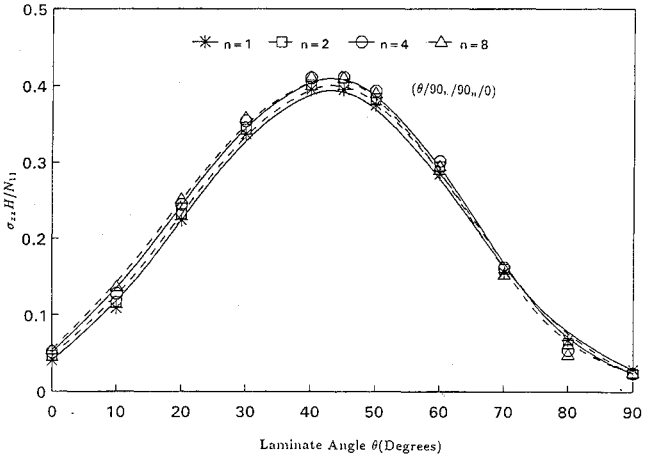

Fig. 9 Interlaminar normal stress σ_{zz} distribution along midplane of $(\theta/90_n/90_n/0)$ laminates under tension.

interval for $n = 1$, 2, 4, and 8. As shown, in Figs. 8 and 9, the highest interlaminar shear stress σ_{1z} occurs at the 20/90 interface of a $(20/90_8/90_8/0)$ laminate. However, the $(45/90_8/90_8/0)$ laminate has the largest interlaminar normal stress σ_{zz}. In addition, it is observed in Fig. 8 that the increase of the number of 90-deg ply groups does not influence σ_{zz} significantly.

IV. Conclusions

The present work presents a method for calculating the interlaminar stresses near the straight free edge. Although a maximum number of plies of 18 was used in the example problems, the method can be used for even thicker laminates without foreseeable difficulty. The current technique is oriented to efficiency and simplicity in analyzing the interlaminar stress distributions near the free edge in generally stacked laminates subjected to different types of loads. This efficient methodology should be used in the preliminary design phase and provides an efficient means to allow engineers to make a selection from a number designs for final consideration.

Appendix: Interlaminar Stresses in General Laminates

The expressions for f_i are given as follows:

$$f_1 = \sum_{k=1}^{N} A_3^{(k)2} \hat{S}_{22}^{(k)} \left(\frac{1}{3} B_1^{(k)2} t^3 + B_1^{(k)} t^2 + t \right)$$

$$f_2 = \sum_{k=1}^{N} A_3^{(k)2} \hat{S}_{33}^{(k)} \left\{ \frac{1}{252} B_1^{(k)2} t^7 + \frac{1}{36} B_1^{(k)2} t^6 + \left(\frac{1}{15} B_1^{(k)} B_3^{(k)} + \frac{1}{20} \right) t^5 + \left(\frac{1}{12} B_1^{(k)} B_4^{(k)} + \frac{1}{4} B_3^{(k)} \right) t^4 + \left(\frac{1}{3} B_3^{(k)2} + \frac{1}{3} B_4^{(k)} \right) t^3 + B_3^{(k)} B_4^{(k)} t^2 + B_4^{(k)2} t \right\}$$

$$f_3 = \sum_{k=1}^{N} A_3^{(k)2} \bar{S}_{44}^{(k)} \left\{ \frac{1}{20} B_1^{(k)2} t^5 + \frac{1}{4} B_1^{(k)} t^4 + \frac{1}{3} \left(B_1^{(k)} B_3^{(k)} + 1 \right) t^3 + B_3^{(k)} t^2 + B_3^{(k)2} t \right\}$$

$$f_4 = \sum_{k=1}^{N} A_5^{(k)2} \bar{S}_{55}^{(k)} \left\{ \frac{1}{20} B_5^{(k)2} t^5 + \frac{1}{4} B_5^{(k)} t^4 + \frac{1}{3} \left(B_5^{(k)} B_7^{(k)} + 1 \right) t^3 + B_7^{(k)} t^2 + B_7^{(k)2} t \right\}$$

$$f_5 = \sum_{k=1}^{N} A_5^{(k)2} \hat{S}_{66}^{(k)} \left(\frac{1}{3} B_5^{(k)2} t^3 = B_5^{(k)} t^2 + t \right)$$

$$f_6 = \sum_{k=1}^{N} A_3^{(k)} \frac{\bar{S}_{12}^{(k)}}{\bar{S}_{11}^{(k)}} \left\{ \frac{-t^3}{3} B_1^{(k)} \left(\bar{S}_{11}^{(k)} b_1^{(k)} + \bar{S}_{12}^{(k)} b_2^{(k)} + \bar{S}_{16}^{(k)} b_3^{(k)} \right) + \frac{t^2}{2} \left[B_1^{(k)} \left(\bar{S}_{11}^{(k)} a_1^{(k)} + \bar{S}_{12}^{(k)} a_2^{(k)} + \bar{S}_{16}^{(k)} a_3^{(k)} \right) - \left(\bar{S}_{11}^{(k)} a_1^{(k)} + \bar{S}_{12}^{(k)} a_2^{(k)} + \bar{S}_{16}^{(k)} a_3^{(k)} \right) \right] + t \left(\bar{S}_{11}^{(k)} a_1^{(k)} + \bar{S}_{12}^{(k)} a_2^{(k)} + \bar{S}_{16}^{(k)} a_3^{(k)} \right) \right\}$$

$$f_7 = \sum_{k=1}^{N} A_4^{(k)} \frac{\bar{S}_{16}^{(k)}}{\bar{S}_{11}^{(k)}} \left\{ \frac{-t^3}{3} B_5^{(k)} \left(\bar{S}_{11}^{(k)} b_1^{(k)} + \bar{S}_{12}^{(k)} b_2^{(k)} + \bar{S}_{16}^{(k)} b_3^{(k)} \right) + \frac{t^2}{2} \left[B_5^{(k)} \left(\bar{S}_{11}^{(k)} a_1^{(k)} + \bar{S}_{12}^{(k)} a_2^{(k)} + \bar{S}_{16}^{(k)} a_3^{(k)} \right) - \left(\bar{S}_{11}^{(k)} a_1^{(k)} + \bar{S}_{12}^{(k)} a_2^{(k)} + \bar{S}_{16}^{(k)} a_3^{(k)} \right) \right] + t \left(\bar{S}_{11}^{(k)} a_1^{(k)} + \bar{S}_{12}^{(k)} a_2^{(k)} + \bar{S}_{16}^{(k)} a_3^{(k)} \right) \right\}$$

$$f_8 = \sum_{k=1}^{N} A_3^{(k)2} \hat{S}_{23}^{(k)} \left\{ \frac{1}{30} B_1^{(k)2} t^5 + \frac{1}{6} B_1^{(k)} t^4 + \frac{1}{3} \left(B_1^{(k)} B_3^{(k)} + \frac{1}{2} \right) t^3 + \frac{1}{2} \left(B_3^{(k)} + B_1^{(k)} B_4^{(k)} \right) t^2 + B_4^{(k)} t \right\}$$

$$f_9 = \sum_{k=1}^{N} A_3^{(k)} A_5^{(k)} \hat{S}_{26}^{(k)} \left\{ \frac{1}{3} B_1^{(k)} B_5^{(k)} t^3 + \frac{1}{2}\left(B_1^{(k)} + B_5^{(k)}\right) t^2 + t \right\}$$

$$f_{10} = \sum_{k=1}^{N} A_3^{(k)} A_5^{(k)} \hat{S}_{36}^{(k)} \left\{ \frac{1}{30} B_1^{(k)} B_5^{(k)} t^5 + \left(\frac{1}{24} B_1^{(k)} + \frac{1}{8} B_5^{(k)} \right) t^4 + \left(\frac{1}{6} + \frac{1}{3} B_3^{(k)} B_5^{(k)} \right) t^3 + \frac{1}{2}\left(B_3^{(k)} + B_4^{(k)} B_5^{(k)}\right) t^2 + B_4^{(k)} t \right\}$$

$$f_{11} = \sum_{k=1}^{N} A_3^{(k)} A_5^{(k)} \bar{S}_{45}^{(k)} \left\{ \frac{1}{20} B_1^{(k)} B_5^{(k)} t^5 + \frac{1}{8}\left(B_1^{(k)} + B_5^{(k)}\right) t^4 + \frac{1}{6}\left(B_3^{(k)} B_5^{(k)} + B_1^{(k)} B_7^{(k)} + 2\right) t^3 + \frac{1}{2}\left(B_3^{(k)} + B_7^{(k)}\right) t^2 + B_3^{(k)} B_7^{(k)} t \right\}$$

in which

$$\hat{S}_{ij}^{(k)} = \bar{S}_{ij}^{(k)} - \bar{S}_{1i}^{(k)} \bar{S}_{1j}^{(k)} \Big/ \bar{S}_{11}^{(k)}$$

and $a_i^{(k)}$ and $b_i^{(k)}$ can be obtained from the following matrix form:

$$\begin{Bmatrix} a_1 \\ a_2 \\ a_3 \end{Bmatrix}^{(k)} = \begin{bmatrix} \bar{Q}_{11} & \bar{Q}_{12} & \bar{Q}_{16} \\ \bar{Q}_{12} & \bar{Q}_{22} & \bar{Q}_{26} \\ \bar{Q}_{16} & \bar{Q}_{26} & \bar{Q}_{66} \end{bmatrix}^{(k)} \begin{Bmatrix} \epsilon_{11}^0 - t_0^{(k)} \kappa_{11} \\ \epsilon_{22}^0 - t_0^{(k)} \kappa_{22} \\ \gamma_{12}^0 - t_0^{(k)} \kappa_{12} \end{Bmatrix}$$

$$\begin{Bmatrix} b_1 \\ b_2 \\ b_3 \end{Bmatrix}^{(k)} = \begin{bmatrix} \bar{Q}_{11} & \bar{Q}_{12} & \bar{Q}_{16} \\ \bar{Q}_{12} & \bar{Q}_{22} & \bar{Q}_{26} \\ \bar{Q}_{16} & \bar{Q}_{26} & \bar{Q}_{66} \end{bmatrix}^{(k)} \begin{Bmatrix} \kappa_{11} \\ \kappa_{22} \\ \kappa_{12} \end{Bmatrix}$$

Acknowledgment

The study was partially supported by the National Science Council of the Republic of China under Grant NSC 82-0401-E005-021.

References

[1]Pipes, R. B., and Pagano, N. J., "Interlaminar Stresses in Composite Laminates under Uniform Axial Extension," *Journal of Composite Materials*, Vol. 4, Oct. 1970, pp. 538–548.

[2]Salamon, N. J., "Interlaminar Stresses in Layered Composite Laminates in Bending," *Journal of Fiber Science and Technology*, Vol. 2, No. 3, 1978, pp. 305–317.

[3]Wang, A. S. D., and Crossman, F. W., "Some New Results on Edge Effect in Symmetric Composite Laminates," *Journal of Composite Materials*, Vol. 11, Jan. 1977, pp. 92–106.

[4]Spilker, R. L., and Chou, S. C., "Edge Effects in Symmetric Composite Laminates: Importance of Satisfying the Traction-Free-Edge Condition," *Journal of Composite Materials*, Vol. 14, Jan. 1980, pp. 2–20.

[5]Chan, W. S., and Ochoa, O. O., "An Integrated Finite Element Model of Edge-Delamination Analysis for Laminates due to Tension, Bending, and Torsion Loads," AIAA Paper 87-0704, April 1987.

[6]Hsu, P. W., and Herakovich, C. T., "Edge Effect in Angle-Ply Composite Laminates," *Journal of Composite Materials*, Vol. 11, Oct. 1977, pp. 422–428.

[7]Wang, J. T. S., and Dickson, J. N., "Interlaminar Stresses in Symmetric Composite Laminates," *Journal of Composite Materials*, Vol. 12, Oct. 1978, pp. 390–402.

[8]Wang, S. S., and Choi, I., "Boundary-Layer Effect in Composite Laminates Part 1—Free Edge Stress Singularities," *Journal of Applied Mechanics*, Vol. 49, Sept. 1982, pp. 541–548.

[9]Kassapoglou, C., and Lagace, P. A., "An Efficient Method for the Calculation of Interlaminar Stresses in Composite Materials," *Journal of Applied Mechanics*, Vol. 53, Dec. 1986, pp. 744–750.

[10]Kassapoglou, C., "Determination of Interlaminar Stresses in Composite Laminates under Combined Loads," *Journal of Reinforced Plastics and Composites*, Vol. 9, Jan. 1990, pp. 33–58.

[11]Jones, R. M., *Mechanics of Composite Materials*, McGraw–Hill, New York, 1970, Chap. 4.